



ELSEVIER

Contents lists available at ScienceDirect

Planetary and Space Science

journal homepage: www.elsevier.com/locate/pss

EURONEAR—Recovery, follow-up and discovery of NEAs and MBAs using large field 1–2 m telescopes [☆]

O. Vaduvescu ^{a,b,c,d,*}, M. Birlan ^{b,e}, A. Tudorica ^{f,g,h,i}, A. Sonka ^{j,k}, F.N. Pozo ^c, A.D. Barr ^c, D.J. Asher ^l, J. Licandro ^{d,m}, J.L. Ortiz ⁿ, E. Unda-Sanzana ^c, M. Popescu ^{b,k,o}, A. Nedelcu ^{b,e}, D. Dumitru ^{h,k}, R. Toma ^{g,h,p}, I. Comsa ^q, C. Vancea ^h, D. Vidican ^k, C. Opriseanu ^k, T. Badescu ^h, M. Badea ^h, M. Constantinescu ^k

^a Isaac Newton Group of Telescopes (ING), Apartado de Correos 321, E-38700 Santa Cruz de la Palma, Canary Islands, Spain

^b IMCCE, Observatoire de Paris, 77 Avenue Denfert-Rochereau, 75014 Paris Cedex, France

^c Instituto de Astronomía, Universidad Católica del Norte (IA/UCN), Avenida Angamos 0610, Antofagasta, Chile

^d Instituto de Astrofísica de Canarias (IAC), C/Vía Láctea s/n, 38205 La Laguna, Spain

^e Astronomical Institute of the Romanian Academy, Cutitul de Argint 5, Bucharest 040557, Romania

^f Bonn Cologne Graduate School of Physics and Astronomy, Germany

^g Argelander-Institut für Astronomie, Universität Bonn, Auf dem Hügel 71 D-53121 Bonn, Germany

^h University of Bucharest, Department of Physics, CP Mg-11, Bucharest Magurele 76900, Romania

ⁱ Institute for Space Sciences, Bucharest - Magurele, Ro-077125, Romania

^j Astronomical Observatory “Admiral Vasile Urseanu”, B-dul Lascar Catargiu 21, Bucharest, Romania

^k Bucharest Astroclub, B-dul Lascar Catargiu 21, sect 1, Bucharest, Romania

^l Armagh Observatory, College Hill, Armagh BT61 9DG, UK

^m Departamento de Astrofísica, Universidad de La Laguna, E-38205 La Laguna, Tenerife, Spain

ⁿ Instituto de Astrofísica de Andalucía (IAA), CSIC, Apt 3004, 18080 Granada, Spain

^o Polytechnic University of Bucharest, Faculty of Applied Sciences, Department of Physics, Bucharest, Romania

^p Romanian Society for Meteors and Astronomy (SARM), CP 14 OP 1, 130170 Targoviste, Romania

^q Babes-Bolyai University, Faculty of Mathematics and Informatics, 400084 Cluj-Napoca, Romania

ARTICLE INFO

Article history:

Received 27 January 2011

Received in revised form

23 June 2011

Accepted 27 July 2011

Available online 4 August 2011

Keywords:

Minor planets

Near Earth asteroids

Main belt asteroids

Orbits

Astrometry

Follow-up

Survey

Discovery

ABSTRACT

We report on the follow-up and recovery of 100 program NEAs, PHAs and VIs using the ESO/MPG 2.2 m, Swope 1 m and INT 2.5 m telescopes equipped with large field cameras. The 127 fields observed during 11 nights covered 29 square degrees. Using these data, we present the incidental survey work which includes 558 known MBAs and 628 unknown moving objects mostly consistent with MBAs from which 58 objects became official discoveries. We planned the runs using six criteria and four servers which focus mostly on faint and poorly observed objects in need of confirmation, follow-up and recovery. We followed 62 faint NEAs within one month after discovery and we recovered 10 faint NEAs having big uncertainties at their second or later opposition. Using the INT we eliminated four PHA candidates and VIs. We observed in total 1286 moving objects and we reported more than 10,000 positions. All data were reduced by the members of our network in a team effort, and reported promptly to the MPC. The positions of the program NEAs were published in 27 MPC and MPEC references and used to improve their orbits. The $O-C$ residuals for known MBAs and program NEAs are smallest for the ESO/MPG and Swope and about four times larger for the INT whose field is more distorted. For the astrometric reduction, the UCAC-2 catalog is recommended instead of USNO-B1. The incidental survey allowed us to study statistics of the MBA and NEA populations observable today with 1–2 m facilities. We calculate preliminary orbits for all unknown objects, classifying them as official discoveries, later identifications and unknown outstanding objects. The orbital elements a , e , i calculated by FIND_ORB software for the official discoveries and later identified objects are very similar with the published elements which take into account longer observational arcs; thus preliminary orbits were used in statistics for the whole unknown dataset. We present a basic model which can be used to distinguish between MBAs and potential NEAs in any sky survey. Based on three evaluation methods, most of our unknown objects are consistent with MBAs, while up to 16 unknown objects could represent NEO candidates and four represent our best NEO candidates. We assessed the observability of the unknown MBA and NEA

[☆] Based on observations taken with the telescopes ESO/MPG 2.2 m in La Silla (ESO Run number 080.C-2003), Swope 1 m in Las Campanas (CNTAC 2008) and the INT 2.5 m in La Palma (CAT DDT 2010).

* Corresponding author at: Isaac Newton Group of Telescopes (ING), Apartado de Correos 321, E-38700 Santa Cruz de la Palma, Canary Islands, Spain.

Tel.: +34 922 425461.

E-mail addresses: ovidiu@ing.iac.es, ovidiu.vaduvescu@gmail.com (O. Vaduvescu).

populations using 1 and 2 m surveys. Employing a 1 m facility, one can observe today fewer unknown objects than known MBAs and very few new NEOs. Using a 2 m facility, a slightly larger number of unknown than known asteroids could be detected in the main belt. Between 0.1 and 0.8 new NEO candidates per square degree could be discovered using a 2 m telescope.

Crown Copyright © 2011 Published by Elsevier Ltd. All rights reserved.

1. Introduction

Near Earth Asteroids (NEAs) are defined as minor planets with a perihelion distance $q \leq 1.3$ AU and an aphelion distance $Q \geq 0.983$ AU (Morbidelli et al., 2002). Potentially Hazardous Asteroids (PHAs) are NEAs having a minimum orbital intersection distance $MOID \leq 0.05$ AU and an absolute magnitude $H \leq 22$ mag (Bowell and Muinonen, 1994). Virtual Impactors (VIs) represent objects for which the future Earth impact probability is non-zero according to the actual orbital uncertainty (Milani and Gronchi, 2009).

According to present data (e.g., [Bowell, 2011](#)), there are more than half a million orbits of known Main Belt Asteroids (MBAs) and about 7600 catalogued NEAs of which about 1200 are PHAs ([NASA and JPL, 2011](#)) and ca 100 VIs ([NEODYs, 2011](#)). During the last two decades the total numbers of discovered NEAs and PHAs have continued to grow, mainly thanks to five dedicated surveys led by the United States (CSS, LINEAR, Spacewatch, LONEOS and NEAT) which have been using large field mostly 1 m class telescopes. Together, they have discovered 86.8% of the entire NEA population known today (MPC January 2011 database), while Europe accounts for less than 1% (led by La Sagra and Crni Vrh mostly run by amateurs). Some European initiatives were taken by national institutions or local collaborations (ASIAGO/ADAS in Italy and Germany, CINEOS in Italy, KLENOT in the Czech Republic, NEON in Finland) and a few programs to study physical properties of NEAs have been carried out by groups in Europe (led by P. Pravec in the Czech Republic, SINEO led by M. Lazzarin in Italy, another program led by J. Licandro in Spain, etc.). Thus although there is still no common European program and no dedicated telescope to observe NEAs, the existence of this expertise, in addition to extensive observational facilities, evidently provides an opportunity for Europe to improve its number of discoveries.

In spite of the larger facilities apparently available today, extremely few researchers have used 2 m class or larger facilities to observe fainter NEAs. During two short runs at ESO La Silla, [Boattini et al. \(2004\)](#) employed the ESO/MPG 2.2 m as a search facility and the NTT 3.5 m as a follow-up telescope to survey faint NEAs and MBAs beyond 22nd magnitude. During three nights using the ESO/MPG facility, the authors incidentally observed about 700 MBAs as faint as $R=21.5$ mag ($V \sim 22$ mag) exposing between 60 and 150 s in the R band. Using only 4 h in override service mode at the Yepun VLT 8.2 m telescope, [Boattini et al. \(2003\)](#) eliminated four very faint VIs ($22 < V < 25$ mag), shifting them to simply the NEA or PHA class.

Although the known NEA and PHA populations have increased during the last few decades, the annual growth of the number of known NEAs and PHAs appears to be becoming constant during recent years ([EARN, 2011](#)), probing some size threshold due to the limiting magnitude $V \sim 21$ mag reached by the present 1 m class surveys. It is unclear whether new 2 m surveys such as the Spacewatch 1.8 m and especially the new Pan-STARRS PS1 1.8 m (although not entirely dedicated to NEAs) will make a significant contribution to the completeness of NEAs through the small size objects.

During the last four years, the European Near Earth Asteroids Research (EURONEAR) program has observed to date 234 program NEAs, defined as NEAs specifically planned to be observed according to a few selection criteria to be discussed below.

Throughout our program, we used 10 mostly 1 m class telescopes, in visiting mode, contributing with follow-up astrometry and recovery of some important NEAs, PHAs and VIs, allowing their orbits to be secured or improved ([Birlan et al., 2010](#)). Part of this work, three telescopes in Chile and the Canaries, represent our largest facilities employed, namely the ESO/MPG 2.2 m in La Silla, Swope 1 m in Las Campanas, and the INT 2.5 m in La Palma, all equipped with large field cameras. To take advantage of these facilities, incidentally to our main program NEA work, we have identified many known MBAs in the observed fields and have also discovered many new objects.

In this paper we review our EURONEAR observations at ESO/MPG and Swope and we present our new observations at the INT. Besides presenting our main NEA follow-up program, we introduce and discuss our incidental survey work using the observed fields, classifying all the observed sources as known MBAs, unknown MBAs and NEA candidates. By comparing the statistics obtained from our survey on the three 1–2 m facilities, and also with those obtained from other authors using 4 and 8 m telescopes, we assess the observability limits of the MBA and NEA populations observable with 1 and 2 m telescopes. In [Section 2](#) of the paper we explain the basic principles driving the planning, observations and data reduction of our runs. In [Section 3](#) we present the results, including program NEAs, known MBAs and other unknown objects. In [Section 4](#) we discuss the results, focusing on the known and unknown MBA and NEA populations, comparing all three facilities and presenting some statistics. The conclusions are presented in [Section 5](#).

2. Observations and data reduction

As part of the EURONEAR project, between 2008 and 2010 we obtained three runs and a total of 11 nights for proposals devoted to the recovery and follow-up of some important NEAs, PHAs and VIs using the ESO/MPG and Swope telescopes in Chile and the INT in La Palma. For each run, the targets were selected based on the daily updated known NEA population.

2.1. Planning the runs

To search and prioritize the objects, we have used four planning servers with which one can check on a daily or hourly basis the updated NEA database. To complement the existing surveys focused on discovery, we focused our EURONEAR runs on some important objects in need of orbital improvement, especially on newly discovered faint asteroids which need to be secured against loss and also on other older objects having a short observed arc which needs to be improved at the second or a later opposition. We selected our targets taking into account the following six criteria:

1. Object class: observe objects classified as VIs, PHAs or NEAs (in this order), to improve their orbits and confirm or change their classification;
2. time interval from discovery: secure and follow-up poorly observed objects, a few days or weeks from discovery;
3. number of oppositions: recover objects previously observed at very few oppositions (especially one-opposition objects);

4. object brightness: recover and follow-up faint and very faint objects, accessible only to larger facilities (larger than 2 m) in danger of being lost by current surveys;
5. positional uncertainty: recover and follow-up poorly observed objects having large positional uncertainty (up to 1°), less accessible to other smaller field facilities; and
6. new object confirmation: recover newly discovered objects, preferably a few to several hours after their discovery.

To implement these criteria, we have used the following four *planning servers*:

1. EURONEAR Planner 1: queries the Spaceguard database for mostly newly discovered objects;
2. EURONEAR Planner 2: queries the MPC Bright and Faint Recovery Opportunity databases for mostly older objects in need of being recovered at a new opposition;
3. MPC NEO Confirmation Page: includes 1-night objects in need of being confirmed by independent observers; and
4. NASA/JPL Close Approaches List: includes closest approaches of old and new objects visible from Earth.

Both EURONEAR (2011) planner web-services are accessible online, being written in PHP by our team and offered to the community for planning other NEA follow-up campaigns. The servers query the current Spaceguard or MPC databases (both updated on a daily basis) and return the prioritized observing lists given the observing place, facility and observing date. The planning is based on eight calculated observability factors, namely: the asteroid class (according to MPC), the apparent magnitude, proper motion, ephemeris uncertainty, altitude, star density in the field, and Moon illumination and distance, calculated with a time step (e.g., 1 h) in a given time interval (e.g., one night). The result consists of a few tables listing at each step the recommended observable objects prioritized according to the object apparent magnitude, its altitude (or airmass), proper motion, sky plane error, or some proposed “Observability” factor calculated as the product of all the above individual observability factors. Two accurate ephemeris servers, namely NEODYs (2011) and IMCCE (2011), are queried by the planning server automatically, returning sky coordinates, magnitudes and uncertainties according to the observed orbital arc. The response time for both servers is short, usually less than 1 min for one night’s information.

2.2. Observations

We present here our observing runs at ESO/MPG in La Silla, Swope in Las Campanas and INT in La Palma.

2.2.1. ESO/MPG observing run

During three nights from 10 to 13 March 2008 we used the ESO/MPG 2.2 m telescope at ESO La Silla, Chile to observe 15 program NEAs, PHAs and VIs. At the Cassegrain $F/5.9$ focus of the telescope we used the Wide Field Imager (WFI) which consists of a 2×4 mosaic of CCDs $2K \times 4K$ pixels each, covering a total field of view of $34' \times 33'$ with a pixel scale of $0.24''/\text{pix}$.

Due to the relatively high proper motion of NEAs at opposition (around $2\text{--}3''/\text{min}$), the average seeing of about $1\text{--}1.5''$, and taking into account the large raw image size on disk (140 MB) combined with the relatively slow readout time compared with our fast planned cadence, we observed the entire run in binning mode 3×3 ($0.71''$ pixel size). We used an R band filter for the entire run. This binning does not affect the quality of our astrometry (set by the goal of having astrometric errors less than

$0.3''$, i.e., comparable with the star catalog reference), as can be observed from the statistics in Section 3.

To take advantage of the large MPG and WFI facility, we focused our run on two aspects, namely to follow-up some important NEAs, and to discover and recover many MBAs appearing in the observed fields. The weather was clear all three nights, with only 2 h lost due to high humidity at the beginning of the first night. The sky was dark, with the Moon 3–6 days past new.

In Table A.1. of our past paper (Birlan et al., 2010) we listed the 15 observed NEAs during our ESO/MPG run, six VIs, four PHAs and five other NEAs. Besides the 15 NEA program fields, during the following available nights we observed nine neighbouring fields, in order to secure some MBAs discovered in the previous nights. The neighbouring fields were chosen assuming a proper motion of $0.7''/\text{min}$ for MBAs observed near opposition. During the second night only, we also surveyed eight WFI fields (2.5 square degrees) in the ecliptic, about 50° from opposition to avoid crowding from the Milky Way. Besides the program NEAs, we identified and measured all moving sources in all the observed fields, reporting all known and new objects visible up to $V \sim 22$ mag. During all three nights at ESO/MPG, we observed in total 42 WFI fields covering about 13 square degrees.

2.2.2. Swope observing run

During five nights on 18–19 October and 22–24 October 2008 we used the Swope 1 m telescope in Las Campanas Observatory (LCO), Chile, to observe 50 program NEAs. At the Cassegrain $F/7$ focus of the telescope we used the *SITe#3* $2K \times 3.6K$ pixel camera giving a field of $15.1' \times 26.5'$ with a pixel scale $0.43''/\text{pix}$. We used an R band filter and no binning for the entire run. The sky was gray (Moon up to 4 days from last quarter) and the weather was very good, with seeing around $1''$.

In Table A.1. of our past paper (Birlan et al., 2010) we listed our 50 observed NEAs during the Swope run, 12 PHAs and 38 other NEAs. Besides the program NEAs, we identified and measured all moving sources in the observed fields, reporting all known and new objects visible up to $R \leq 20.4$ mag. During five nights we observed in total 50 Swope fields covering some 6 square degrees.

2.2.3. INT observing runs

During two discretionary nights (D-nights) on 12 February and 15 April 2009 (3+3 h), 1 h in 13/14 November 2009 and four nights awarded by the Spanish Director’s Discretionary Time (DDT) in 20–25 February and 3 March 2010, we used the INT 2.5 m telescope in Roque de Los Muchachos Observatory (ORM) in La Palma to observe 35 program NEAs, namely one VI, 13 PHAs and 21 other NEAs. At the prime focus of the INT we used the Wide Field Camera (WFC) which consists of four CCDs $2K \times 4K$ pixels each, covering an L-shape $34' \times 34'$ with a pixel scale of $0.33''/\text{pix}$. Both D-nights and 13/14 November 2009 were observed without binning, while the February–March 2010 run was observed with 2×2 binning ($0.66''/\text{pix}$) to minimize the readout time and match the poor weather conditions. We used an R filter for all runs.

Most of the INT time was bright and gray, with only 3 h dark time. The weather was good during the first 6 h on the first two D-nights and 1 h in 13/14 November 2009, but very bad (wet and windy) during the whole DDT run (February–March 2010) when the Moon was gray and bright. In Table 1 we list the INT program NEAs, including the object classification, proper motion, 3σ positional uncertainty (according to the MPC for the observing date) and the orbital arc length at the observing date. Besides the program NEAs, at the INT we identified and measured all moving sources in all observed fields, reporting all known and new objects visible up to $R \sim 21.2$ mag. In total at the INT, we observed for about three clear nights, a total of 35 WFC fields covering some 10 square degrees.

Table 1

The observing log for NEA observations at INT. We list the name of the asteroid, its classification at time of observation, date of observation, expected apparent magnitude V , exposure time (s), number of observed positions, apparent motion μ ("/min), ephemeris uncertainty (arcsec) and observed orbital arc since discovery (d-days, m-months, y-years). Objects marked with * represent special cases discussed in the paper.

Asteroid	Class	Date (UT)	V (mag)	Exp (s)	Nr pos	μ ("/min)	3σ (")	Obs arc
2009 CW1	NEA	2009 February 12	19.9	20	10	3	40	9d
2009 CB2*	?	2009 February 12	20.1	60	5	3	1000	6d
2009 CA2	NEA	2009 February 12	20.0	30	8	1	30	9d
2003 SJ84*	NEA	2009 February 12	21.4	120	5	2	81	6y
2009 FF	PHA	2009 April 15	20.8	60	5	2	38	1m
2009 DZ	PHA	2009 April 15	21.1	120	6	1	3	1m
2009 FJ30	NEA	2009 April 15	17.8	30	5	5	9	18d
2009 FT	NEA	2009 April 15	19.2	30	6	4	1	18d
2009 FJ44	PHA	2009 April 15	19.5	60	5	1	2	16d
2009 FG19	PHA	2009 April 15	20.5	90	5	2	24	25d
2009 FH44	NEA	2009 April 15	19.8	60	5	2	1	16d
2009 FY4	PHA	2009 April 15	21.0	120	10	1	12	26d
2009 FV4	NEA	2009 April 15	21.1	90	5	1	26	26d
2009 FR30	NEA	2009 April 15	21.2	120	4	1	56	20d
2009 FT32	NEA	2009 April 15	20.8	30	5	11	42	24d
2009 VR25*	VI	2009 November 13	20.7	30	4	5	1400	2d
2009 VN1	NEA	2009 November 14	21.0	30	5	7	932	5d
2009 VQ	NEA	2009 November 14	20.9	30	5	7	3	6d
2009 KK	PHA	2009 November 14	21.2	60	5	2	270	6m
2010 DJ1*	NEA	2010 February 20	19.3	30	5	10	190	3d
2010 CF55	NEA	2010 February 20	20.8	90	3	3	39	5d
2010 CF12*	NEA	2010 February 20	19.8	90	2	10	?	8d
2010 DX1	NEA	2010 February 23	17.9	30	5	8	24	4d
2010 DF1	PHA	2010 February 23	20.5	60	4	3	94	6d
2007 RM133*	NEA	2010 February 23	21.4	120	5	1	490	3y
2000 SV20*	NEA	2010 February 25	21.0	120	4	1	2900	10y
2010 DC*	NEA	2010 March 03	20.1	120	8	1	58	17d
2009 FY4	PHA	2010 March 03	16.8	10	5	12	1	1y
2007 EF*	PHA	2010 March 03	18.2	10	8	20	1	3y
2000 CO101	PHA	2010 March 03	16.3	20	6	6	1	10y
2008 EE	NEA	2010 March 03	16.5	20	7	6	1	2y
2006 SS134	PHA	2010 March 03	20.5	20	3	12	2	4y
2010 DJ56	PHA	2010 March 03	20.9	180	4	2	3	11d
2007 JZ20	NEA	2010 March 03	20.8	180	5	1	1	3y
2008 TZ3	PHA	2010 March 03	21.1	120	7	2	1	2y

2.3. Data reduction

For all runs, we processed the data within 2–3 days from observations using an IRAF pipeline (for the INT and Swope data) and IDL (for ESO/MPG data), taking into account the usual subtraction of the appropriate bias and sky flat field. For the WFI and WFC mosaic cameras we sliced CCD images and treated them independently, calculating CCD centres based on the pointing of the telescope (included in the image headers) and the geometry of the two cameras. All images were processed on-site, then archived and eventually transferred via FTP to the remote available data reducers, allocated on demand.

In order to secure some unknown objects, we observed at ESO/MPG nine fields in multiple nights, seven imaged during two nights and two fields during three nights. To identify objects observed in multiple nights, we extrapolated in time the arcs of all moving sources observed during the first night using a least square fitting code written by our team. By comparing the extrapolated positions of objects observed in one field during the first night for the observing date corresponding to the second night with the positions of the objects observed in the follow-up field during the second night, one could easily pair objects in the α – δ position space. In case of crowding and close matches, the magnitude represents a second indicator. Using this pairing technique we matched all the unknown objects observed during multiple nights, namely 43 objects observed during two nights and eight objects observed during three nights. Thanks to this

confirmation, most of these objects became credited discoveries. Fig. 1 presents an example of such identification of objects observed in a crowded field (9° from opposition and 4° south of the ecliptic). With cyan circles we plot predicted positions and with magenta circles observed positions.

The reduced images were analysed and measured using Astrometrica (Raab, 2011), carefully visually blinking all images of the same field in order to detect all moving objects. Around 100 reference stars (UCAC-2 for Swope data or USNO-B1 for ESO/MPG and INT data) were used for each CCD to perform the astrometry, using a linear model in the cases of WFI and Swope known to have small field distortion and fitting a 3-degree polynomial in the case of WFC to accommodate its larger optical field distortion. According to the literature and also to our derived astrometry (Section 3.1), the astrometric errors due to the field distortion appear very small for the WFI field, being mostly within $0.1''$ across most of the WFI field (about 90%), according to the field distortion pattern derived by Assafin et al. (2010) which shows the largest distortion in the corners of the mosaic (up to $0.53''$) and some distortion around $0.2''$ in the upper and lower edge and the centre of the mosaic. Relative photometry was derived by Astrometrica using from a dozen to a few hundred catalog stars visible in the field, the reduced asteroid magnitudes having an uncertainty of about 0.1 mag. For all runs, we decided to use Astrometrica in preference to other software because of its simplicity, common platform and simple installation and usage by all members of the team, as many of the data reducers were

students and amateurs. We inspected the data visually instead of using automated software, because of the relatively low volume of data per run, and mostly because the human eye and brain are known to detect faint moving sources better than the computer. We detected asteroids as low as ca 1.5σ level from noise, which allowed us to recover many faint targets inaccessible to other automated surveys.

All the reduced data (output of Astrometrica in MPC format) were collected by the PI of the run, checked for errors using the EURONEAR $O-C$ calculator or the FITSBLINK residual calculator (Skvarc, 2010a), then submitted to the MPC in three groups: the

observed NEAs, the known asteroids, and the unknown asteroids (possibly discovered by us).

3. Results

During all three runs, we observed effectively in total about 11 nights, reporting positions and magnitudes for 100 program NEAs (seven VIs, 29 PHAs and 64 NEAs), 558 known MBAs and 628 unknown moving objects, in total 1286 objects observed in 29 square degrees total surveyed field.

Table 2 presents the overview of our observations at ESO/MPG, Swope and INT, listing the number of observed objects, number of reported positions and the standard deviation of the orbital fit using our data (according to NEODYs). We classify the objects in three groups: observed NEAs, known MBAs, and the unknown (unidentified) objects. We further classify the unknown objects in three groups: official discoveries, later identifications and outstanding objects. We include the number of nights observed at each facility, the number of observed fields, the total sky coverage (in square degrees) and the limiting magnitude for each facility. Next, we give the total number of objects. Finally, we conclude with some density statistics which will be discussed in Section 4.4.

3.1. Program NEAs

In the left panels of Figs. 2–4 we plot the $O-C$ residuals (observed minus calculated) in α and δ for the program NEAs observed at ESO/MPG, Swope and INT, based on the orbital fits available on 22 November 2010 (NEODYs, 2011). The $O-C$ standard deviations are $0.15''$ for the ESO/MPG dataset, $0.39''$ for Swope and $0.42''$ for the INT.

In total, 27 MPC and MPEC publications include data from our three runs. Table 3 includes these references: 12 publications containing our Swope observations, 10 our ESO/MPG observations and six publications including our INT data.

Birlan et al. (2010) presented the most important NEAs recovered at ESO/MPG and Swope. At ESO/MPG we observed 12 faint objects (six VIs, three PHAs and three NEAs) less than one month after

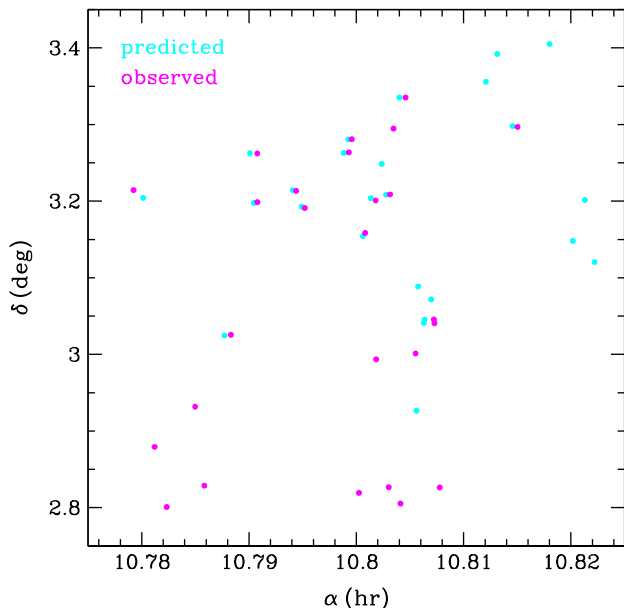


Fig. 1. Pairing the unknown objects observed in multiple nights based on positions derived from the extrapolated arc. Cyan points stand for extrapolated positions of objects observed in the first night and magenta points mark objects observed in the second night in the follow-up field. (For interpretation of the references to color in this figure legend, the reader is referred to the web version of this article.)

Table 2

Summary of the ESO/MPG, Swope and the INT runs.

Observations	ESO/MPG	Swope	INT	Total
Program NEAs	15	50	35	100
Nr of positions	156	506	169	831
$O-C$ standard deviation ($''$)	0.15	0.39	0.42	–
Known MBAs	347	68	143	558
Nr of positions	2976	680	733	4389
$O-C$ standard deviation ($''$)	0.15	0.18	0.66	–
Unknown objects	467	41	120	628
Nr of positions	4183	261	574	5019
Official discoveries	58	0	0	58
Later identifications	17	8	22	47
Outstanding objects	392	33	98	523
Nr. of nights	3	5	3	11
Nr. of observed fields	42	50	35	127
Sky coverage (square degrees)	13	6	10	29
Limiting magnitude (R)	21.5	20.4	21.2	–
Total nr. of objects	829	159	298	1286
Total nr. of positions	7315	1447	1476	10,239
Known MBAs density (obj/sq.deg)	27	11	14	–
Unknown MBAs density	36	7	12	–
Unknown NEOs density	0.2–0.6	0	0.1–0.8	–

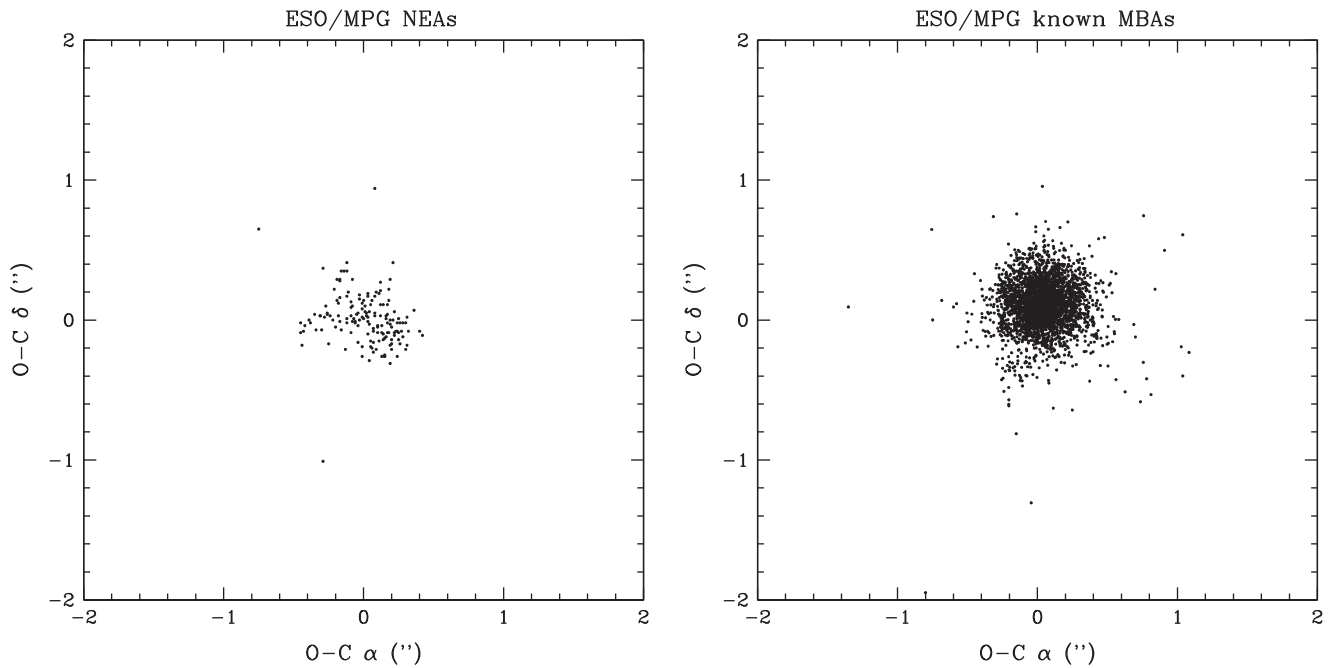


Fig. 2. $O-C$ (observed minus calculated) residuals for program NEAs and known MBAs observed at ESO/MPG.

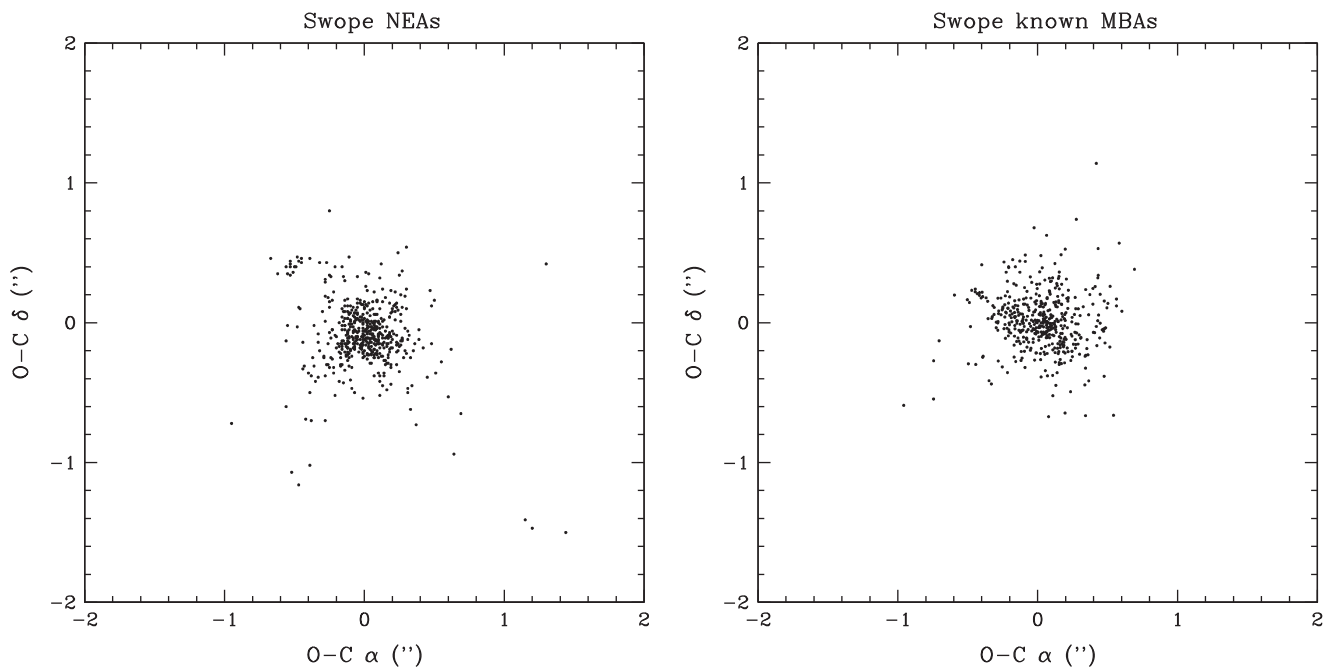


Fig. 3. $O-C$ (observed minus calculated) residuals for program NEAs and known MBAs observed with Swope telescope.

discovery, and also recovered two faint objects (one PHA and one NEA) at their second or later opposition. With Swope we observed 25 objects (all NEAs) soon after discovery, recovering also two objects (one NEA and one PHA) at their second or later opposition. From Table 1 we can count the number of recoveries using the INT: 25 objects soon after discovery (one VI, eight PHAs and 16 NEAs) and six faint objects having large uncertainty recovered at their second or later opposition (two PHAs and four NEAs).

Nine especially important NEAs were observed with the INT. We mark them with * in the first column of Table 1 and we discuss them next. Thanks to the large aperture of the INT and the large field of the WFC, we eliminated three NEA candidates and one VI. First classified as a NEA, 2009 CB2 had a poor orbit

(2 day arc) and a very high sky uncertainty ($3\sigma = 1000''$). Thanks to the large field of WFC, we recovered this object one week later, allowing its orbit to be improved and eliminating it from the NEA list. A similar case was 2010 CF12, originally classified as a NEA based on a small 3 day arc. Although the MPC did not list its sky uncertainty by the time of our INT run, we recovered this object one week later and eliminated it from the NEA list. Another object degraded from the NEA class to the MBA class was 2010 DC. It had a small arc based on four nights data and a sky uncertainty of about $1'$, allowing fast recovery two weeks later at the INT. One of the most important detections of the INT was 2009 VR25, a new object classified as a VI based on its original poor two night orbit. Although quite faint ($V=20.7$ mag) and having very large sky

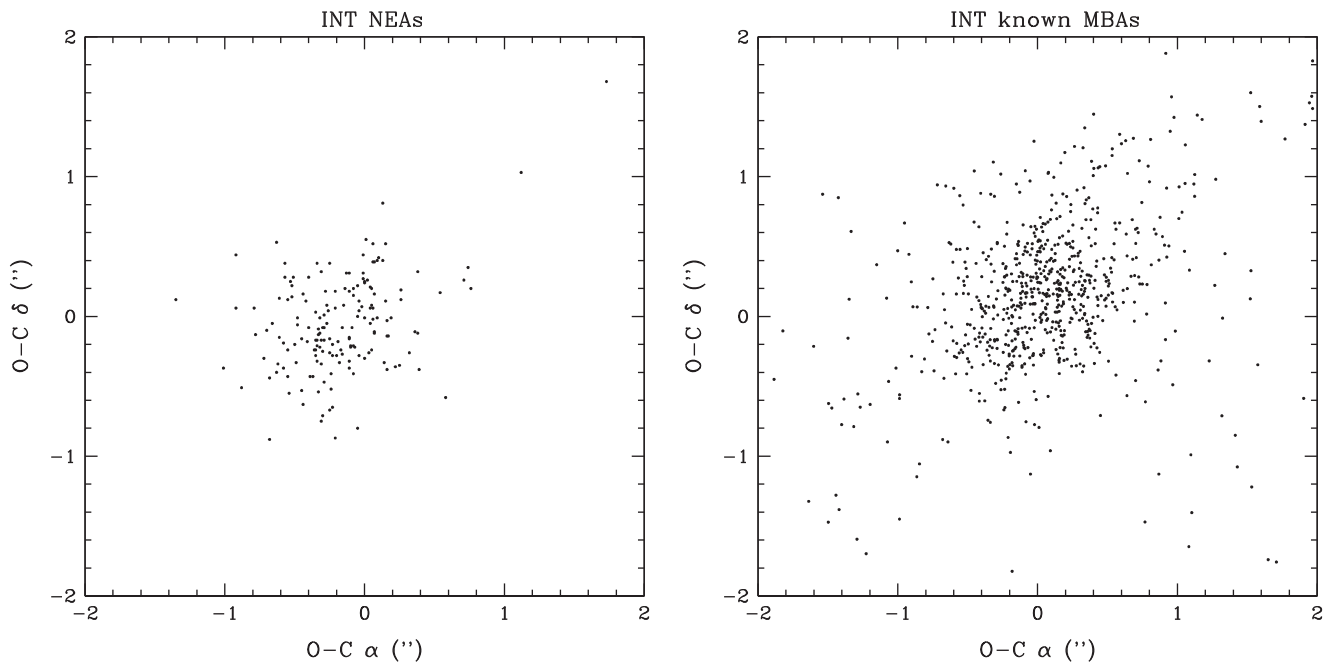


Fig. 4. $O-C$ (observed minus calculated) residuals for program NEAs and known MBAs observed with the INT.

Table 3

Minor Planet Circulars (MPC) and Minor Planet Electronic Circulars (MPEC) publishing our NEA observations.

Telescope	MP(E)C	Reference
Swope	MPC 64484, 5	Benecchi et al. (2008a)
Swope	MPC 64096, 9	Benecchi et al. (2008b)
Swope	MPC 66688, 10	Benecchi et al. (2009a)
Swope	MPC 64753, 3	Benecchi et al. (2009b)
Swope	MPC 63365, 10	Kern et al. (2008)
Swope	MPC 66190, 11	Kern et al. (2009)
Swope	MPEC 2008-U48	Pozo et al. (2008)
Swope	MPEC 2008-U46	Scotti et al. (2008a)
Swope	MPEC 2008-U45	Scotti et al. (2008b)
Swope	MPEC 2008-K66	Tubbiolo et al. (2008)
Swope	MPC 63125, 6	Vaduvescu and Tudorica (2008)
Swope	MPEC 2008-K63	Young et al. (2008)
ESO/MPG	MPC 63369, 9	Cavadore et al. (2008)
ESO/MPG	MPC 63591, 10	Elst et al. (2008a)
ESO/MPG	MPC 63129, 5	Elst et al. (2008b)
ESO/MPG	MPC 62871, 8	Elst et al. (2008c)
ESO/MPG	MPC 62573, 3	Elst et al. (2008d)
ESO/MPG	MPC 66195, 4	Elst et al. (2009a)
ESO/MPG	MPC 65331, 2	Elst et al. (2009b)
ESO/MPG	MPC 65045, 7	Elst et al. (2009c)
ESO/MPG	MPC 62258, 1	Sheppard et al. (2008)
ESO/MPG	MPC 62262, 5	Tholen et al. (2008)
ESO/MPG	MPC 65636, 2	Tholen et al. (2009)
INT	MPC 66196, 2	Holman et al. (2009)
INT	MPEC 2010-E39	Holvorcem et al. (2010)
INT	MPC 66457, 4	Fitzsimmons et al. (2009a)
INT	MPC 65927, 9	Fitzsimmons et al. (2009b)
INT	MPC 65332, 1	Fitzsimmons et al. (2009c)

uncertainty ($3\sigma = 1400''$), we could find it, enabling its reclassification from the VI to NEA class.

We recovered three NEAs at their second opposition with the INT. 2007 RM133 was discovered in 2007, having a short arc (one month) at the time of the INT run. Despite its very faint magnitude ($V=21.4$ mag) and very large sky uncertainty ($3\sigma = 490''$), we recovered it 3 years later, allowing a substantial

improvement of its orbit (Holvorcem et al., 2010). Another second opposition recovery was 2003 SJ84, another NEA observed for only one month, following its discovery in 2003. Although very faint ($V=21.4$ mag) and having quite large positional uncertainty ($3\sigma = 81''$), we recovered it six years later about $21'$ away from its predicted position (15 times more than its nominal MPC 3σ value) and we improved its orbit (Fitzsimmons et al., 2009c). Our best ever second opposition recovery was 2000 SV20. This NEA was observed for 3 months following its discovery in 2000 and recovered 10 years later by the INT/WFC about $7'$ away from its predicted MPC position (7 times more than the nominal MPC $3\sigma \sim 1'$ value).

Using the INT, in 2010 we followed two Arecibo radar targets. 2010 DJ1 was requested by NASA in February 2010 (Benner, 2010), having an uncertainty ($3\sigma = 190''$) which allowed its INT recovery only three days after discovery. 2007 EF was another Arecibo target, moving very fast ($\mu = 20''/\text{min}$) but allowing successful WFC imaging at $V=18.2$ mag in only 10 s exposures.

3.2. Known MBAs

During all three runs in the observed program NEA fields, we observed incidentally a total of 558 known MBAs.

In the right panels of Figs. 2–4 we plot the $O-C$ residuals for the known MBAs observed in all three runs based on their current orbits available at 22 November 2010 (AstDyS, 2011). The standard deviations are $0.15''$ for the ESO/MPG dataset, $0.18''$ for Swope and $0.66''$ for the INT.

The standard deviations of the ESO/MPG dataset for both NEAs and MBAs are very small, proving the excellent quality of this telescope equipped with the WFI which allowed very accurate astrometry across its whole large field. Nevertheless, a systematic offset to the north of $0.111'' \pm 0.001''$ in δ and $0.037'' \pm 0.001''$ in α shows up in the right panel of Fig. 2 for the known MBA dataset observed at ESO/MPG, with the observed median position located north-west of the calculated ephemerides. This effect is consistent with results of Tholen et al. (2008a) who found a surprising systematic offset of the astrometry of the asteroid Apophis of about $0.2''$ based on 200 observations reduced with the USNO-B1

catalog (which was also used by us to reduce our ESO/MPG data). By comparing USNO-B1 with ICRF, the authors determined for the USNO-B1 an average declination offset of $+0.116''$, in perfect agreement with our findings.

The standard deviation of the Swope datasets is $0.39''$ for the NEA data and $0.11''$ for the MBA data, and no sample shows any systematic offset with respect to the origin. We reduced Swope data with the UCAC-2 catalog, known to have better astrometry than USNO-B1. Both for Swope and ESO/MPG runs, the standard deviation for the MBA sample is smaller than that of the NEA sample probably because of the higher S/N due to brighter and slower moving MBA objects, compared with the fainter and faster moving program NEAs.

The INT/WFC shows relatively large residuals for both NEA and MBA samples (up to about $2''$ and standard deviation $0.66''$ as quoted above) and only for this facility the deviation of the MBA sample is larger than that of the program NEAs. Bad weather did not impede the astrometry for our INT run, catalog stars being quite bright in a 2 m telescope resulting in good S/N and sub-arcsec stellar positions. The USNO-B1 catalog has an average astrometric accuracy of $0.2''$, too small to explain the larger residuals of the INT astrometry. The larger residuals for known MBAs than for program NEAs observed with INT/WFC can, however, be explained taking into account that MBAs were imaged across the entire WFC field which is heavily affected by the field distortion at the INT prime focus, compared with the central CCD#4 where most of the NEAs were observed and the WFC field has the smallest distortion. Given this, for any future INT/WFC work we plan to correct the image field before data reduction.

3.3. Unknown objects

A total of 467 unknown moving objects were identified at ESO/MPG, 41 at Swope and 120 at the INT (Table 2). The observed proper motion for most objects was compatible with MBAs with a few exceptions discussed next.

Throughout our paper and in Table 2 we classify the unknown objects in three categories: *official discoveries* (confirmed by the MPC according to their DISCSTATUS monthly list), *later identifications* (unknown objects which could be linked with existing arcs) and *outstanding objects* (waiting for orbital links from independent observations, possibly to be credited to us later).

3.3.1. Unknown MBAs

We include in the Appendix A (available only in the online version of our paper) seven tables listing all the unknown objects observed at ESO/MPG (Tables A.1–A.3), Swope (Tables A.4 and A.5) and the INT (Tables A.6 and A.7). We give first the official discoveries, then later identifications and finally outstanding objects.

Table A.1 includes our official discovered asteroids at ESO/MPG. We give first the EURONEAR object acronym (based on the initials of the surname of the observers and reducers¹), then the official designation (from the MPC), three main orbital parameters (semi-major axis a , eccentricity e and inclination i), Earth minimum orbital intersection distance $MOID$, absolute magnitude H , number of observed positions, arc length (in days or years), rms of the $O-C$ residuals for the orbital fit σ , observed apparent magnitude R , ecliptic latitude β , Solar elongation ε (both in degrees) and apparent proper motion μ (in $''/min$). We distinguish directions

east and west of opposition by letting ε increase above 180° for fields to the east.

For each object we give in the first line the orbital elements fitted with the FIND_ORB software (Gray, 2011a) based on our observations only and for the standard epoch $MJD = 54520.0$. On the second line we list the orbital elements taken from the MPC database (Minor Planet Center (MPC), 2011) calculated by fitting all MPC available observations for an epoch close to the mid-point interval of those observations.

Table A.2 includes the unknown objects (at the date of the run) which were identified later (in November 2010) with known objects, based on the checks of the MPC database and the MPC automatically assigning designations. Our calculated orbits, presented again in the first line, are based on the very short available arc (observations acquired in less than 1 h), and so should be regarded with caution.

For both official discoveries and later identified objects, the orbital elements from the first line are very close to the official elements in the second line. Although most of our fits are based on very short arcs observed during 1–3 nights at ESO/MPG and only one night at Swope and INT, one can observe the success of the FIND_ORB fit for most objects, especially for the a , e and i parameters which will be used in statistics later. In particular, based on 116 paired orbits available from the three runs, we can compare FIND_ORB versus MPC by calculating the median values of the differences in a , e , i and H , which are 0.20 AU, 0.06, 1.05° and 0.70 mag, respectively.

Table A.3 includes the remaining unknown objects observed at ESO/MPG which could not be identified according to the present MPC database (November 2010). For them we give only our calculated orbits, based on very short arcs observed only in one night. The exact elements should be regarded with caution but are usable for statistics in Section 4.

Table A.4 lists the later identified objects observed with the Swope telescope, while Table A.5 gives the outstanding unknown objects observed with Swope. Similarly, Tables A.6 and A.7 give the later identified objects and outstanding unknown objects observed at the INT.

According to the MPC (January 2011 DISCSTATUS), our ESO/MPG run produced 58 official discoveries. Most of the people involved in EURONEAR work on a voluntary basis and include students and amateur astronomers based in Romania. Indeed, the entire ESO/MPG team included people of Romanian origin who became the first Romanian discoverers of minor planets (Vaduvescu, 2009). Given these, in 22 December 2008 we proposed to the Working Group for Small Body Nomenclature (CSBN) of the International Astronomical Union (IAU) a list including 12 Romanian names. In January 2011 the first two of our discovered asteroids received numbers, namely (257,005)=2008 EW152=VBTU207 (our acronym) and (263,516)=2008 EW144=VBTU224, being eligible for naming.

3.3.2. NEO candidates

In this section we will use three tools to check all our unknown objects for potential Near Earth Objects (NEOs). In Table 4 we include all NEO candidates derived from all three methods, marking in bold the best candidates. Besides the observed properties (quantities μ , ε , R , number of positions and $O-C$ standard deviation), we include in this table the orbital parameters (a , e , i) and data derived from the three methods ($MOID$ in column 4, MPC score in column 10 and the Model in the last column).

For the first method we plot in Fig. 5 the apparent proper motion μ versus the Solar elongation ε for all the unknown objects observed at ESO/MPG (red), Swope (green) and the INT (blue). Observed in a given field near opposition (close to $\varepsilon \sim 180^\circ$), MBAs

¹ VB=Vaduvescu and Birlan; TU=Tudorica; SO=Sonka; OP=Opriseau; VI=Vidican; TO=Toma; and VA=Vanacea.

Table 4
Near Earth Object (NEO) candidates—fast unknown objects observed at ESO/MPG (first group) and the INT (second group). We list in bold four objects which qualify as the best NEO candidates, having small MOIDs, 100% NEO Rating score and fitting best the $\varepsilon-\mu$ model. The two one-nighter objects marked with * are not NEAs according to their later identifications.

Acronym	μ ("/min)	ε (deg)	R	MOID (AU)	a (AU)	e	i (deg)	Nr pos	σ (")	MPC score	Model
VB011	0.55	125	20.8	0.19	2.28	0.49	6.7	8	0.13	14	Close
VBTU203	0.65	132	20.8	0.75	1.84	0.05	23.5	16	0.26	10	Fit
VBTU197	0.68	135	21.4	0.09	3.02	0.68	8.2	7	0.38	100	Best
VBVA002	0.60	154	19.8	0.57	2.50	0.39	13.8	3	0.08	22	Fit
VBTU222	2.12	162	20.4	0.03	1.01	0.08	2.2	5	0.16	100	Best
VBTU226	0.89	162	21.0	0.56	1.94	0.20	25.7	5	0.52	21	Fit
VBSO072	1.17	184	20.0	0.70	1.95	0.13	17.5	8	0.12	24	Fit
VBV1213	7.17	191	~20	0.07	2.46	0.57	2.0	7	0.31	100	Best
VITB01	0.43	92	20.1	2.25	3.28	0.01	21.1	5	0.26	77	Bad
VTD069	0.60	151	20.5	0.51	3.01	0.52	10.2	4	0.51	6	Fit
VIT005 *	0.95	167	19.0	0.38	2.66	0.20	14.0	4	0.38	28	Fit
VTD010	1.02	177	20.2	0.97	2.63	0.26	21.3	5	0.30	5	Fit
VTU021	4.61	173	18.9	0.02	1.03	0.02	2.1	3	0.43	100	Best
VTD003 *	1.15	193	19.3	0.35	2.43	0.14	3.3	4	0.35	100	Fit
VTU031	0.90	202	20.5	0.92	1.99	0.03	19.6	5	0.14	10	Fit
VTU028	0.72	202	20.6	0.30	2.39	0.46	7.2	3	0.26	15	Fit
VBA003	0.45	219	21.1	0.79	1.80	0.02	23.5	5	0.08	18	Fit
VTU020	0.67	228	20.3	0.58	1.84	0.14	22.0	6	0.31	25	Fit

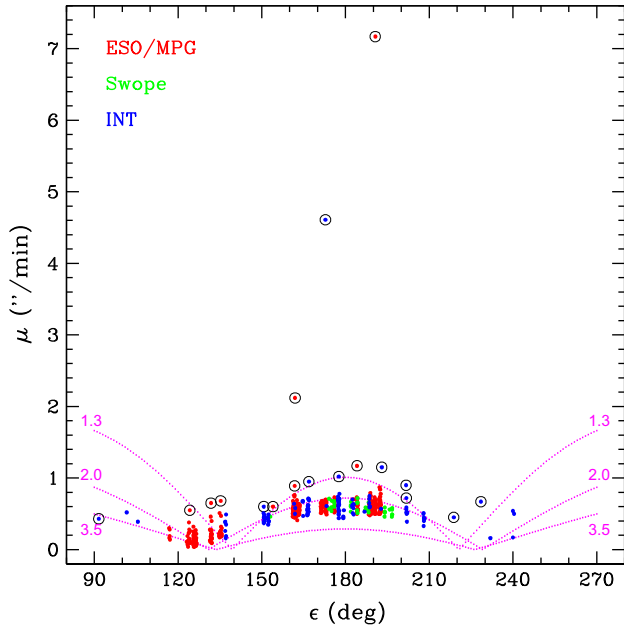


Fig. 5. Basic orbital model using the asteroid observed proper motion μ and the solar elongation ε . We plot all unknown objects observed at ESO/MPG (red), Swope (green) and INT (blue). The three overlaid dotted magenta curves correspond to asteroids orbiting between $a=2.0$ and $a=3.5$ AU (Main Belt) and $a=1.3$ (Near Earth Objects limit). The model allows us to easily flag NEO candidates in a survey. We mark with circles our NEO candidates and we include their properties in Table 4. (For interpretation of the references to color in this figure legend, the reader is referred to the web version of this article.)

are expected to show proper motions distributed in a small vertical “finger”-shaped region with proper motions between $\mu \sim 0.3-0.7$ "/min, depending on their location in the main belt. Observed further away from opposition, MBAs should show smaller proper motions owing to the larger distance and velocity projection effect. Both μ and ε represent quantities measured directly from observations, not being affected by the uncertain orbits derived from the short arc. Therefore, the $\mu-\varepsilon$ plot represents an important method to search a survey for fast moving objects including NEAs, PHAs and other NEOs.

Let us consider the very basic orbital model which assumes the (prograde) asteroid orbit circular and coplanar with the circular

orbit of Earth, and the asteroid at least 90° away from the Sun. Following Kolena (1999) we express the asteroid proper motion as a function ε . Let Δ be the angle between the directions of Sun and asteroid as seen from Earth (Δ is ε or $360^\circ-\varepsilon$, with $0 < \Delta < 180^\circ$). Let v_E and v_a be the orbital velocities of Earth and asteroid, ϕ the angle as seen from the asteroid between the direction of Earth and that of the asteroid’s orbital motion, and E the difference 180° minus the angle (as seen from Earth) between the direction to the asteroid and the direction of Earth’s orbital motion (so $E = \Delta - 90^\circ$). Then the angular speed of the asteroid ω as seen from Earth is the difference in the projected velocities perpendicular to the Earth–asteroid direction, divided by the Earth–asteroid distance:

$$\omega = \frac{v_a \sin \phi - v_E \sin E}{d} \tag{1}$$

From the sine law applied to the triangle Sun–Earth–asteroid:

$$\sin \phi = \sqrt{1 - \frac{a_E^2 \sin^2 \Delta}{a_a^2}} \tag{2}$$

The cosine rule applied to the same triangle, solving the resulting quadratic for d , gives

$$d = a_E \cos \Delta + \sqrt{a_a^2 - a_E^2 \sin^2 \Delta} \tag{3}$$

where we dropped the minus solution because d should always be positive. Kepler’s third law (assuming Earth and asteroid masses very small compared with Sun’s mass) implies $v_a = \sqrt{GM_S/a_a}$ and $v_E = \sqrt{GM_S/a_E}$ where $G=6.673 \times 10^{-11} \text{ m}^3 \text{ kg}^{-1} \text{ s}^{-2}$ is the gravitational constant, $M_S=1.989 \times 10^{30} \text{ kg}$ the Sun’s mass and $a_E=1.496 \times 10^{11} \text{ m}$ the Earth’s semimajor axis.

Substituting all these terms in Eq. (1), and since $\sin E = -\cos \Delta$, we obtain the following formula for the apparent angular speed of the asteroid as a function of Δ and a_a :

$$\omega = \frac{\sqrt{\frac{GM_S}{a_a}} \sqrt{1 - \frac{a_E^2 \sin^2 \Delta}{a_a^2}} + \sqrt{\frac{GM_S}{a_E}} \cos \Delta}{a_E \cos \Delta + \sqrt{a_a^2 - a_E^2 \sin^2 \Delta}} \tag{4}$$

Finally, the proper motion of the asteroid μ in arcsec per minute can be calculated from the angular speed ω in radians per second:

$$\mu = \omega \times \frac{180 \times 3600}{\pi} \times 60 \tag{5}$$

We can use Eq. (5) and the asteroid semimajor axis a_a as a model to map the expected limits for the proper motion of MBAs (defined between $a_a=2.0$ and $a_a=3.5$ AU). In the context of this basic orbital model where we consider proper motions (as a function of elongation) only, we may also represent NEOs by considering orbits with $a_a < 1.3$ AU. By plotting the values of μ between solar elongations 90° and 270° (e.g., using 1° step in ε), one can draw the limits corresponding to these populations. In Fig. 5 we plot with dotted magenta lines the curves corresponding to these limits. The curves are symmetric about 180° (in fact symmetry properties of sky motions hold more generally in the non-coplanar case; see Section 2.1 of Jedicke (1996)).

According to Fig. 5, most of the 628 unknown objects agree with our model, in the sense that most are consistent with asteroids from the main belt. They are located at the bottom of the plot around $\mu=0.2\text{--}0.8''/\text{min}$ and between the two dotted curves corresponding to $a_a=2.0$ and $a_a=3.5$ AU. About 16 objects (2.5% of the total) marked with circles rise above the $a=1.3$ NEO limit and above the main vertical group at the respective elongation. We mark these objects with “fit” or “best” in the last column of Table 4, treating them as potential NEOs. One can clearly distinguish three major outliers showing the fastest proper motions, namely VBVI213 at $\mu=7.17''/\text{min}$ and VBTU222 at $\mu=2.12''/\text{min}$ observed at ESO/MPG, and VTU021 at $\mu=4.61''/\text{min}$ observed at the INT. We mark them with “best” in the last column of Table 4, treating them as our best NEO candidates.

The fastest object was recorded under the acronym VBVI213 and it moved about 10 times faster than all other MBAs observable close to opposition, so it represents our best NEO candidate. This object was clearly visible on 8 CCD images, leaving a 20 pixel trail owing to the relatively long 2 min exposures. It moved in the opposite direction and about 10 times faster than all other asteroids visible in the same field. In Fig. 6 we include the image of this field (CCD#5 of WFI), presenting the corresponding eight frame animation in the online electronic version of the paper. The image is displayed in normal sky orientation and the field of view is about $8' \times 16'$ (one WFI CCD), with pixel size $0.714''$ (in 3×3 binning). Four MBAs marked with circles are visible moving to the upper right, while the NEA candidate is visible as a trail in the bottom part (enlarged twice in the left corner inset). The exposure time was 2 min and the cadence between frames was 3.3 min.

Most of our fields were observed near opposition ($150^\circ < \varepsilon < 210^\circ$) and all agree well with our model. In Fig. 5 there are about three fields located farther from opposition between $130^\circ < \varepsilon < 140^\circ$ for which most unknown objects do not match our model which does not hold due to our basic (circular and coplanar) orbital assumptions (proper motions in the model are close to zero, whereas the real orbits give a small but noticeable component to the proper motions).

Our second NEO search method uses the “NEO Rating” tool developed by the Minor Planet Center (MPC) which calculates a score for possible NEOs based on the expected proper motion of the MBA population distribution (Minor Planet Center (MPC), 2011). Running this tool for all unknown ESO/MPG objects, we obtained NEO scores (“No-ID” probabilities) of 100% for three objects: VBTU197, VBTU222 and VBVI213 which confirm our findings using the first model. Running the NEO Rating for all unknown INT objects we confirm with 100% score two INT objects, VTU021 and VTD003, plus VITB01 with a relatively high score (77%). We plot with circles all these NEO candidates in Fig. 5 and we include the scores in Table 4. All other objects from all runs received very low MPC rates (smaller than 5%), consistent with our MBA classification derived from our model.

Our third NEO search method uses the calculated MOID derived from the preliminary orbits derived with FIND_ORB. The

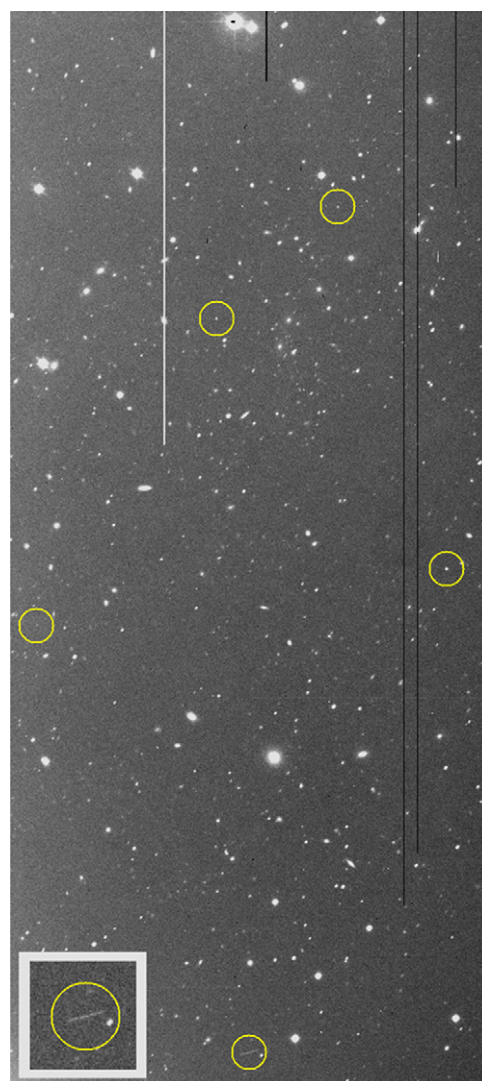


Fig. 6. VBVI213, our best NEO candidate, at the bottom of the $8' \times 16'$ ESO/MPG WFI CCD#5, moving in the opposite direction to the four MBAs marked above, and about 10 times faster. The image is displayed in normal sky orientation (N up, E left) and the inset zooms in on the NEO candidate. An animation including all eight available frames is available online.

results are included in Table 4 and they mostly agree with the other two methods, showing in most cases the reliability of the derived preliminary orbits, especially for the objects observed closed to opposition.

Unfortunately most NEO candidates were observed in only one night and only one object was reobserved during a second night, namely VBTU203=2008 EN144. Two NEA candidates observed at INT were identified later with known objects, namely VTD003=2010 CJ33 and VIT005=2000 SN27. Based on their updated observed arcs, they are not NEAs, so we mark them by * in Table 4. Dropping them from the list, we count in total 16 NEO candidates; this number should be considered an upper bound. Four objects have MPC scores of 100%, small MOIDs (less than 0.1 AU) and they agree mostly with our model, so they represent our best 4 NEO candidates: VBVI213, VBTU222, VBTU197 (observed at ESO/MPG) and VTU021 (observed at the INT). We write their acronyms in bold in the first column of Table 4. There was no NEO candidate observed with Swope, checking all three methods.

We checked the remote possibility that some NEO candidates could be identified with Earth artificial satellites or space debris.

In this sense, we checked all our observed fields against known Earth satellites by using the satellite identification server developed by Skvarc (2010b) based on the software SAT_ID of Gray (2011b). No satellite with proper motion slower than $0.25''/\text{min}$ (corresponding to geostationary orbits) was found within 1° of any observed fields. Known and unknown space debris could also be studied statistically, according to Schildknecht (2007). Compared with NEO candidates, space debris move at very fast speed with angular velocities ranging from a few arcsec per second (i.e., a few arcmin per minute, at least 10 times faster than our fastest NEO candidate) to more than 1000 arcsec per second with respect to the stellar background. Thus, we drop any possibility that any of our unknown objects could be associated with artificial satellites or space debris.

4. Discussion

4.1. Comparison with the known asteroid population

We compare the major orbital parameters of all unknown objects observed at ESO/MPG, Swope and INT with the entire known asteroid population at 10 December 2010 (541,260 orbits) based on the ASTORB database (Bowell, 2011).

In Fig. 7 we plot two classic asteroid orbital distributions, namely e versus a (left) and i versus a (right). We overlay in colours all the unknown objects observed in our survey, including official discoveries, later identifications (based on MPC orbits) and outstanding objects (based on FIND_ORB orbits). One can easily observe that the majority of our objects fit both orbital distributions very well, marking the four major Kirkwood gaps and a few known families. Only 105 points represent our official discoveries and later identifications, while 523 points represent outstanding objects (five times more). Because outstanding objects have orbits calculated with FIND_ORB, at least statistically this confirms the ability of FIND_ORB to calculate preliminary orbits based on very small arcs.

4.2. Comparison between facilities

In Fig. 8 we plot the distribution of the observed apparent magnitude R (left panel) and the calculated absolute magnitude H versus semimajor axis a for all unknown asteroids observed with ESO/MPG, Swope and INT. The limiting magnitude of each system is evident by the levels in the R plot above which the regions become depleted of data. For each fixed limiting R , we expect a negative trend of H versus a , as seen in the right panel. We observed unknown MBAs up to $a \sim 3.3$ AU, which is considered about half the outer main belt region (Yoshida and Nakamura, 2007). As expected, both 2 m facilities sampled well the middle region ($2.6 \leq a \leq 3.0$) and the first half of the outer region ($3.0 \leq a \leq 3.3$), while well over half of unknown objects sampled with the Swope 1 m are in the inner region of the main belt ($2.0 \leq a \leq 2.6$). Moreover, according to Table 2, both ESO/MPG and INT discovered about the same number of MBAs as the number of known MBAs. Thus, a 2 m survey could bring an important contribution to knowledge of the main belt, being expected to double the present number of known MBAs to more than one million.

According to the $O-C$ plots for known MBAs (right panel of Figs. 2–4) and to the $O-C$ standard deviation of $0.15''$ for both NEA and known MBA datasets, ESO/MPG appears to have the best astrometry required for accurate follow-up, recovery and discovery across the whole WFI camera. With standard deviations of $0.18''$ for the known MBA dataset and $0.39''$ for the NEAs, the Swope telescope represents an adequate 1 m facility for asteroid studies at limiting magnitude $R \sim 20.5$ mag. The field of the INT/WFC appears the most distorted, these $O-C$ positions showing the widest spread in Fig. 4 and a standard deviation about 4 times larger compared with the other two facilities. Although the INT astrometry is acceptable around the centre of WFC and could be used to follow-up known objects expected to appear close to the centre, the INT field should be corrected in order to reach more accurate astrometry across the entire WFC field.

Comparing the position of the centroid of the known bulk of MBAs with respect to the calculated positions, we conclude that the USNO-B1 catalog is less appropriate for astrometric reduction

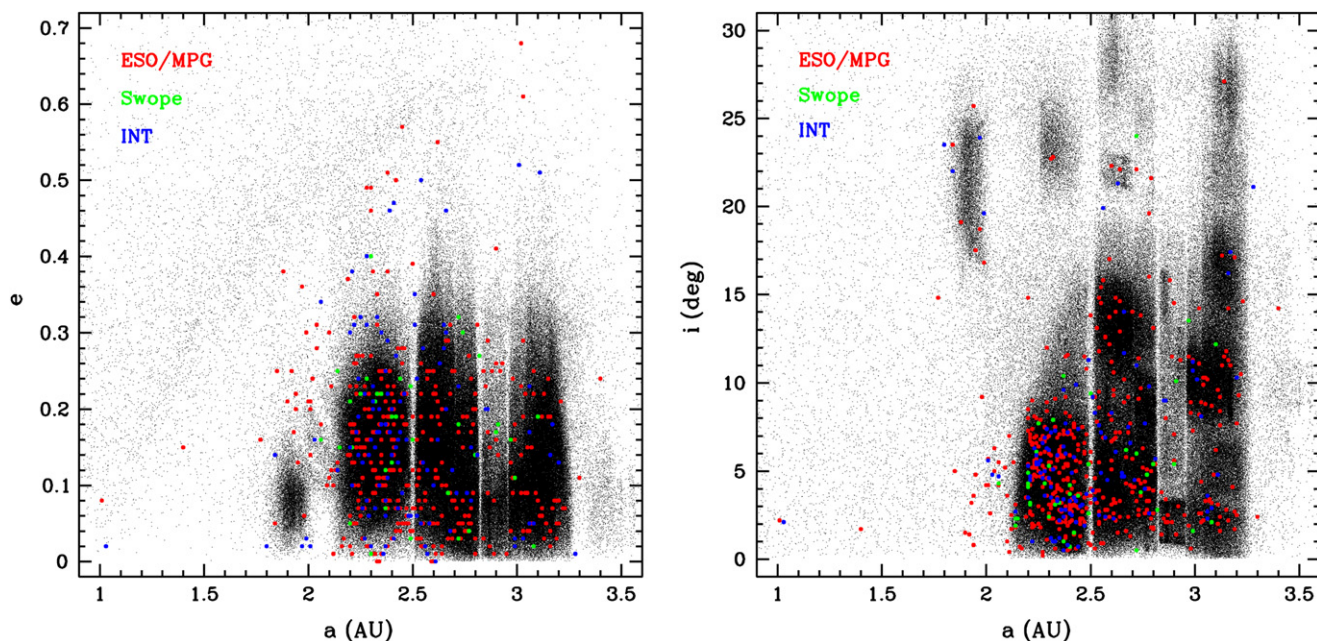


Fig. 7. Orbital distributions of 628 unknown objects observed at ESO/MPG (red points), Swope (green) and INT (blue) compared with the entire known asteroid population (ASTORB - 541,260 fine black points). Although our preliminary orbits were derived using mostly short arcs, the distributions are consistent with the known MBA population, showing the usefulness of the FIND_ORB orbital fit in a , e and i . (For interpretation of the references to color in this figure legend, the reader is referred to the web version of this article.)

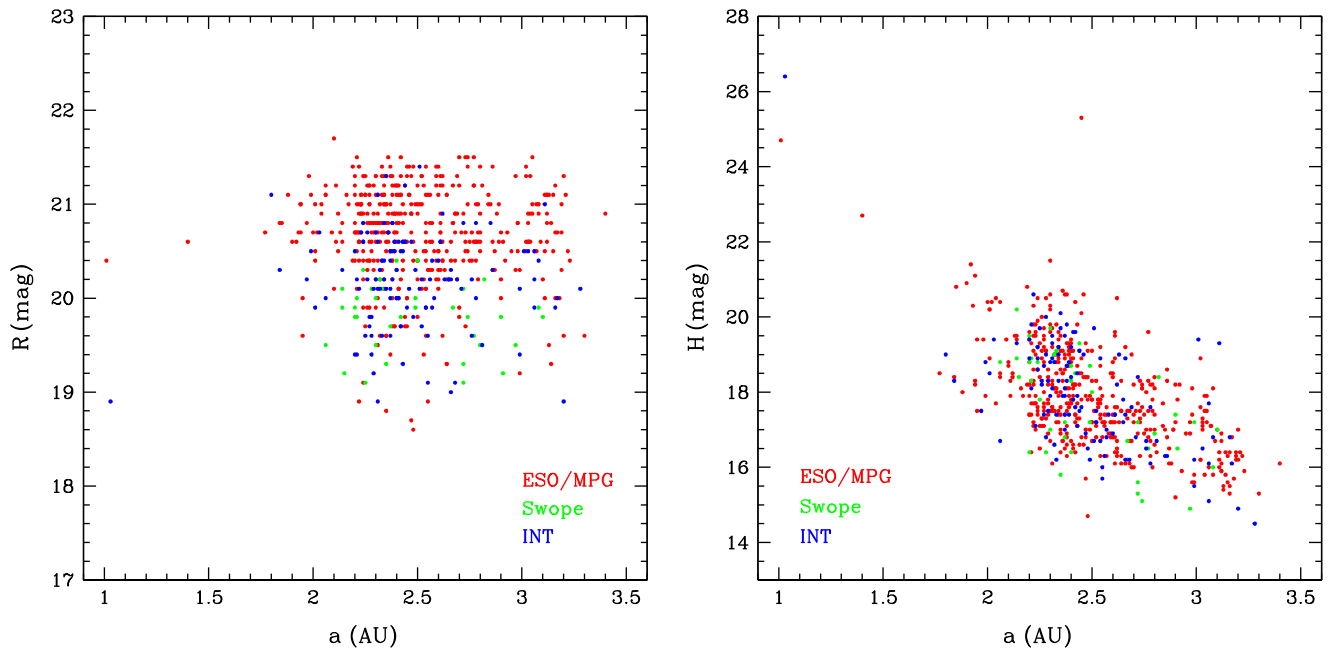


Fig. 8. The observed apparent R magnitude (left) and calculated absolute magnitude H (right) versus the semimajor axis a for the ESO/MPG unknown asteroids dataset (red points), Swope (green) and INT (blue). The three objects having the faintest H are among the best NEO candidates. (For interpretation of the references to color in this figure legend, the reader is referred to the web version of this article.)

due to larger residuals, and we recommend instead UCAC-2 or UCAC-3 which appear to give more accurate results and therefore to be the current best representation of the Hipparcos frame up to magnitude 16. Nevertheless despite the superior accuracy from using the UCAC system, it still has shortcomings for the astrometry of fast moving objects such as the limited north declination coverage of UCAC-2 and the faulty northern proper motion system of UCAC-3.

4.3. Distribution of the unknown MBA and NEO candidates

With the original 1 m Spaceguard survey approaching its goal and limits, new 2 m surveys such as Pan-STARRS will soon take over, increasing the detection limits in both size and depth in the Solar System. Based on our ESO/MPG and INT data, we briefly evaluate here the limits of such a 2 m survey.

The left panel of Fig. 9 plots the histogram showing the observed apparent magnitude R for all the unknown objects observed at ESO/MPG (red colour), Swope (green), the INT (blue) and the total (black dots). Apparently, the dark time at ESO was most efficient to detect unknown objects at $R \sim 20.6$ mag, allowing a limit $R \sim 21.5$ mag. This detection limit is consistent with the actual 1.8 m Pan-STARRS 1 which is expected to reach $R \sim 22$ mag (Grav, 2009). The INT reached maximum detection at $R \sim 20.2$ mag and a more shallow cutoff at $R \sim 21.2$ mag, about 0.3 mag less faint than ESO/MPG despite its larger aperture, probably due to the worse observing conditions at the INT. The 1 m Swope reached a maximum detection at $R \sim 19.8$ mag and a limiting magnitude at $R \sim 20.4$ mag, about one magnitude lower than other 2 m facilities. We include these limits in Table 2.

The right panel of Fig. 9 plots the histogram showing the calculated absolute magnitude H for the unknown objects observed at the three facilities. Five objects fall outside the H range of the plot, namely the brightest object VB037 identified as the jovian Trojan 2001 TB234 ($H=13.3$) and the faintest four objects VBTO016 ($H=22.7$), VBTU222 ($H=24.7$), VBVI213 ($H=25.3$) and VTU021 ($H=26.4$). The last four are visible as clear individual points in Fig. 8 (right) and the last three are among our

best NEO candidates (Table 4). The H histograms are more evenly distributed, showing 2–3 maxima (possibly not all real) for each facility and an overall maximum at $H \sim 17.4$ mag. This limit can be regarded as the limiting H giving completeness for a 2 m class facility for the entire main belt (including the outer region). According to Yoshida and Nakamura (2007), this limit corresponds to S-class asteroids about 1 km in diameter, thus virtually all S-type MBAs larger than this limit should be accessible to a 2 m telescope (including ESO/MPG and INT) in good weather conditions.

As we saw in Fig. 8 (left), $R \sim 21.6$ mag represents the limiting apparent magnitude for the ESO/MPG. Most MBAs have absolute magnitudes between $15 < H < 21$ mag, consistent with sizes between 170 m and 6 km, assuming albedos between 0.05 and 0.25 (NASA and JPL, 2011). The four best NEO candidates have the following H and sizes, assuming the same limits for their albedos: VTU021: $H=26.4$ mag, 13–31 m; VBVI213: $H=25.3$ mag, 22–55 m; VBTU222: $H=24.7$ mag, 30–70 m; VBTU197: $H=18.9$ mag, 440–980 m.

In the left panel of Fig. 10 we plot the calculated MOID versus the elongation ϵ for the unknown objects observed at ESO/MPG (red), Swope (green) and INT (blue). With a dotted line we mark the $\text{MOID} = 0.3$ limit for NEAs below which all our NEO candidates appear. Based on this plot, there is no apparent favorable elongation to discover NEOs.

In the right panel of Fig. 10 we plot the calculated MOID versus the observed ecliptic latitude β for the unknown objects observed at ESO/MPG (red), Swope (green) and INT (blue). Most unknown objects and NEO candidates were observed at low latitudes, under 10° . Most NEO candidates are observed at low latitudes and there is no particular favorable detection latitude with respect of the MBAs.

4.4. Survey statistics for 2 and 1 m facilities

Based on the statistics available from our ESO/MPG, Swope and INT surveys, we can evaluate the unknown MBA and NEA

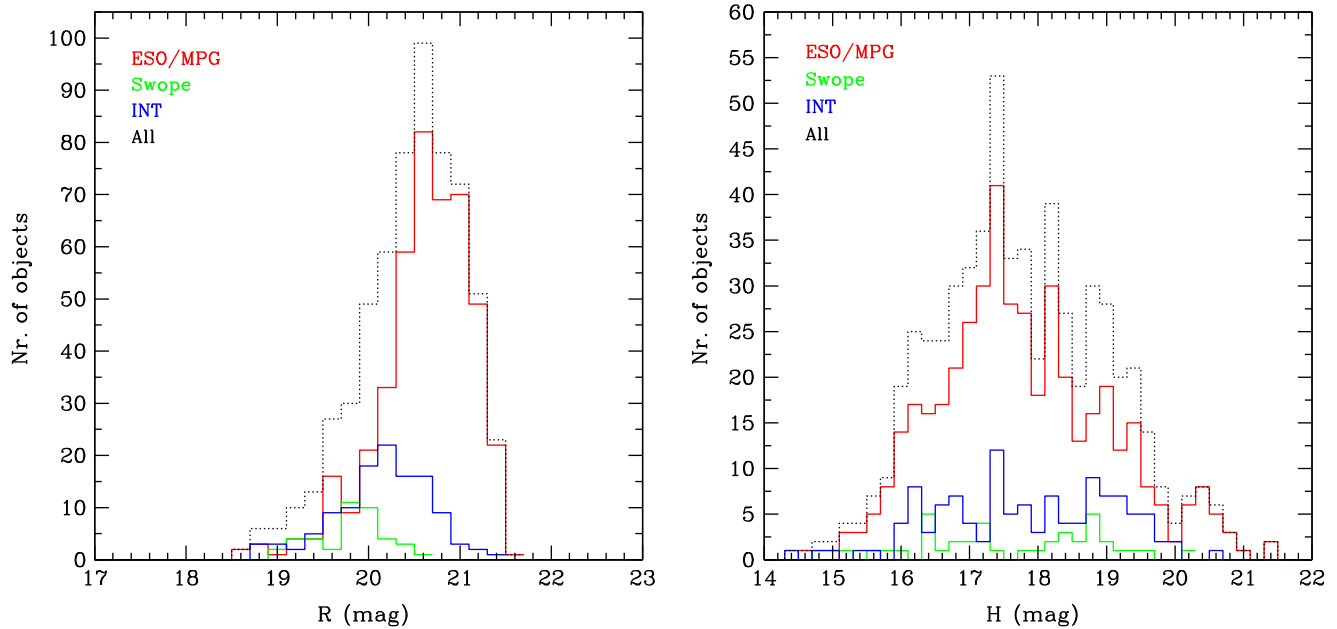


Fig. 9. Histograms showing number of unknown objects as function of observed apparent R magnitude (left) and calculated absolute magnitude H (right) for the ESO/MPG dataset (red), Swope (green), INT (blue) and the total number of objects (black dots). (For interpretation of the references to color in this figure legend, the reader is referred to the web version of this article.)

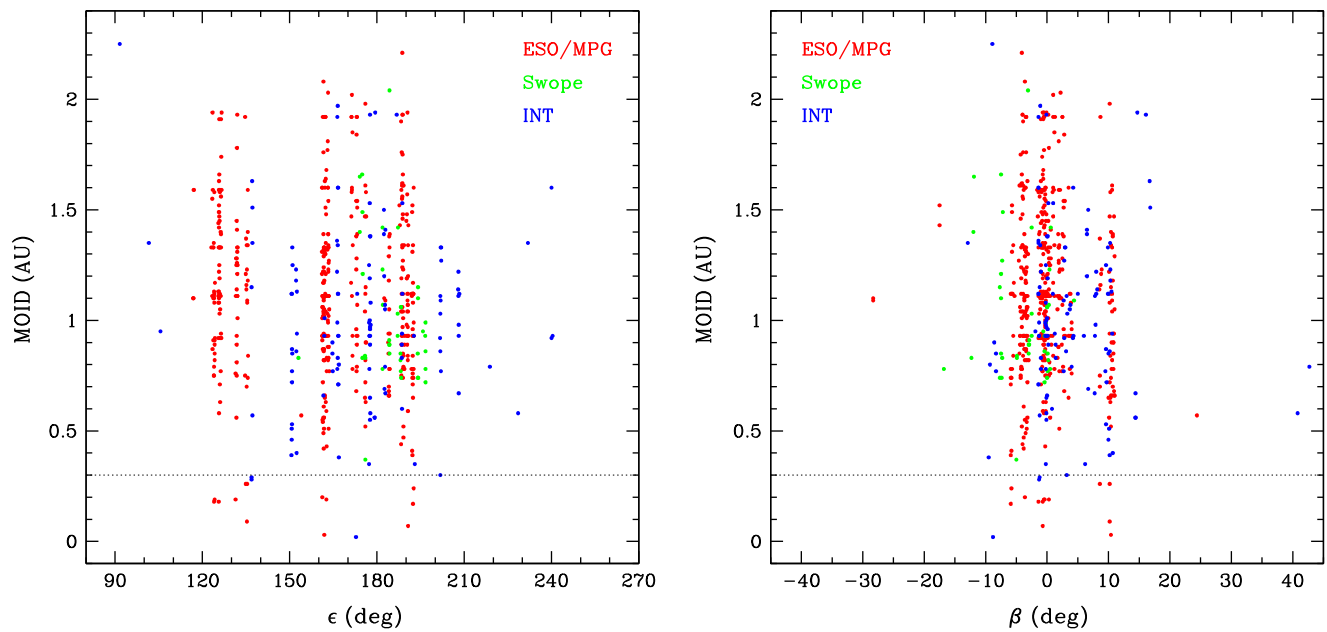


Fig. 10. Minimal Orbital Intersection Distance (MOID) versus Solar elongation ϵ (left panel), and versus ecliptic latitude β (right panel) for the unknown objects observed at ESO/MPG (red), Swope (green) and INT (blue). The dotted line at $MOID < 0.3$ marks the NEO region under which all our NEO candidates appear. (For interpretation of the references to color in this figure legend, the reader is referred to the web version of this article.)

population observable at low latitudes ($|\beta| < 10^\circ$) by 2 and 1 m surveys. We include these results in Table 2.

4.4.1. Unknown MBA density

Using data from our ESO/MPG survey (the best performing 2 m facility) we observed in the 10° latitude range 347 known objects and 467 unknown objects scanning 13 square degrees. This gives an average of 27 known and 36 unknown MBAs per square degree visible to limiting magnitude $R \sim 21.5$ mag in 2 min exposure time using the ESO/MPG. We include these findings at the end of Table 2. These numbers give for ESO/MPG a MBA ratio

known:unknown=0.7. We compare below our findings with other authors.

Counting data from our Swope survey we observed 35 unknown objects and 65 known objects within 10° latitude range from the ecliptic scanning about 5 square degrees of sky. This gives an average of 11 known objects and 7 unknown objects per square degree visible to limiting magnitude $R \sim 20.4$ mag in 2 min exposure time with a 1 m facility. The total number agrees with earlier results from the Spacewatch 0.9 m which detected for the whole survey 16 asteroids per square degree.

Boattini et al. (2004) conducted a three night pilot search and follow-up program to detect NEAs using the ESO/MPG with WFI

in 3×3 binning mode (i.e., same facility and setup as us). During the last two nights, the authors scanned in good weather conditions a total of 24 square degrees, counting an average of 10 known and 12 unknown asteroids (mostly MBAs) per square degree. This gives a ratio known:unknown=0.8 which is consistent with our findings. Nevertheless, both their numbers are about three times less than our findings. Their survey strategy was a bit different than ours, namely they observed at small solar elongation during the first and last part of the night and observing near opposition during the middle part. Also, for identification they used mostly automated software, although some data were reduced with Astrometrica. It is well known that the eye and brain are better than computer software in detection of moving objects by a factor of $\frac{3}{2}$ based on experience of Spacewatch II (Boattini et al., 2004) or by 1–1.5 mag according to other authors (Yoshida et al., 2003). Both these factors could explain the lower density of asteroids (mostly MBAs) found by Boattini et al. (2004) compared with our statistics.

Wiegert et al. (2007) searched 50 fields (50 square degrees) from the CFHT Legacy Survey (CFHTLS 3.6 m) observed in r' close to opposition and within a 2° latitude range from the ecliptic. The moving objects were detected automatically by using the SExtractor software with a threshold 3σ . The authors found an average of 70 asteroids per square degree up to $r' \sim 21.5$ mag (Wiegert, 2011), which agrees well with our findings.

Using the Subaru 8.3 m telescope equipped with the large field SuprimeCam with 7 s exposures Yoshida et al. (2003) surveyed 3 square degrees near opposition and the ecliptic (SMBAS I survey) and found 92 asteroids per square degree to limiting magnitude $R=21.5$ mag. Using the same facility to image 4 square degrees using 2 s exposures (SMBAS II survey), Yoshida and Nakamura (2007) found an average of 75 objects per square degree to the same limit. In these surveys, moving objects were detected by human inspection. Our findings using the ESO/MPG are very close to their densities, taking into account our lower S/N due to Subaru's larger aperture and their pointing at lower latitudes.

Using one single 8.4 m mirror of the Large Binocular Telescope (LBT), Ryan et al. (2009) studied the asteroid distribution in the ecliptic, finding up to $V=22.3$ mag (close to $R \sim 21.5$ mag our limit) a density of 85 asteroids per square degree. Asteroid detection was performed visually using a three-color method. Their density found is very close to ours, counting our total number of objects (63 objects per square degree).

4.4.2. Unknown NEA density

Counting the NEO candidates from Table 4, ESO/MPG produced eight NEO candidates and three best NEO candidates scanning a field of 13 square degrees. This gives between 0.2 and 0.6 NEO candidates per square degree observable with this facility. The value 0.6 is an upper limit because we could not confirm our objects which were observed only in one night.

Scanning 40 WFC fields (13 square degree) within 15° latitude in good weather at ESO/MPG, Boattini et al. (2004) discovered three NEA candidates (including two confirmed NEAs), which gives a density of 0.2 NEA candidates per square degree, matching our findings counting only the best candidates. Comparing their results with those from the 1.8 m Spaceguard II survey, the authors conclude that on average one NEA per 10 square degrees could be discovered with ESO/MPG and the WFI. This is consistent with our findings if we count only one object, namely our best NEA candidate, VBVI213. Counting all our NEO candidates, our result is 6 times more optimistic than that of Boattini et al. (2004).

According to Table 4, INT produced 8 unknown objects and only one best NEA candidate scanning a field of 10 square degrees. This gives between 0.1 and 0.8 NEO candidates per square degree observable with INT (mostly in bad conditions).

These densities are similar with those found by ESO/MPG and consistent with any other 2 m survey.

5. Conclusions

We have analysed our observations taken with the ESO/MPG 2.2 m in La Silla, the Swope 1 m in Las Campanas and the INT 2.5 m in La Palma. The total sky surveyed during 11 nights was about 29 square degrees, which allowed us to study statistics of MBAs and NEAs observable nowadays by other 1–2 m facilities. Our main conclusions are:

- These telescopes are successful at following up faint objects soon after discovery, preventing their loss, recovering NEAs at their second or later opposition and eliminating NEA candidates and Virtual Impactors.
- The majority of our unknown objects are consistent with MBAs, based on two evaluation methods. Up to 16 unknown objects could represent NEO candidates from which 4 represent our best NEO candidates according to three evaluation methods.
- The $O-C$ residuals for known MBAs and program NEAs amount to $0.15''$ for the ESO/MPG, $0.39''$ and $0.18''$ for Swope and $0.42''$ and $0.66''$ for the INT, whose prime focus field is the most distorted (especially the three non-central CCDs) and needs to be corrected in order to improve the astrometry.
- The UCAC-2 catalog is better than USNO-B1 which shows an offset of $0.1''$ to the North, consistent with previous findings of other authors.
- Published orbits (specifically a , e and i) of known asteroids are very similar to our calculated orbits using the FIND_ORB software based on our observed very small arcs.
- Based on statistics derived from our data, we could assess the observability of the unknown MBA and NEA populations using 1m and 2 m class surveys. Employing a 1 m facility one can observe today fewer unknown objects than known MBAs and virtually no new NEO. Using a 2 m facility, a slightly larger number of unknown than known MBAs could be detected (up to about $a=3.2$ AU), consistent with objects having sizes between 170 m and 6 km (taking into account the limits of the main belt and the albedo range). Between 0.1 and 0.8 new NEO candidates per square degree could be discovered using a 2 m telescope.
- A basic model assuming circular and coplanar orbits of the asteroids and Earth could be used in order to check any large all sky survey for potential NEO candidates. Employing the proper motion and Solar elongations, this model does not depend on calculated quantities such as orbital elements possibly subject to errors. Compared with other tools such as the MPC's NEO Rating and the calculated preliminary orbits, this model seems very accurate at small elongations ($\pm 30^\circ$ from opposition) but, based on the residuals in our data, smaller elongations (around $120-140^\circ$) need further study.

Acknowledgements

This work was based on observations made with the ESO/MPG telescope at La Silla Observatory under programme ID 080.C-2003(A), the Swope telescope at Las Campanas Observatory (CNTAC 2008), both granted under Chilean time, and the INT telescope in La Palma under Director's Discretionary Time of Spain's Instituto de Astrofísica de Canarias (CAT DDT 2010). OV acknowledges ESO, LCO and IA/UCN for supporting the runs in Chile for himself and the students, and also to the ING, IAC and the IAA for supporting the run in La Palma for the students.

OV and JL gratefully acknowledge support from the Spanish “Ministerio de Ciencia e Innovación” (MICINN) project AYA2008-06202-C03-02. This research has made intensive use of the Astrometrica software developed by Herbert Raab, very simple to install and use by students and amateur astronomers. We also used the image viewer SAOImage DS9, developed by Smithsonian Astrophysical Observatory and also IRAF, distributed by the National Optical Astronomy Observatories, operated by the Association of Universities for Research in Astronomy, Inc. under cooperative agreement with the National Science Foundation. Special thanks are due to Bill Gray for providing FIND_ORB and installation assistance. OV also acknowledges to Paul Wiegert for feedback necessary to compare MBA data observable with CFHT and the ESO/MPG telescopes. Thanks are due to Fumi Yoshida and Tsuko Nakamura for sharing their SMBAS data and interest. We also acknowledge to Jure Skvarc for his satellite identification software and to Lilian Dominguez for providing some references about space debris. Thanks are also due to Alain Maury who helped us to count NEA discoveries made in Europe. Acknowledgements are due to the referee whose constructive suggestions helped us to improve the paper.

Appendix A. Supplementary data

Supplementary data associated with this article can be found in the online version at doi:10.1016/j.pss.2011.07.014.

References

- Assafin, M., et al., 2010. *Astronomy & Astrophysics* 515, A32.
- AstDyS, 2011. Asteroids Dynamic Site: <<http://hamilton.dm.unipi.it/astdys/>>.
- Benecchi, S., Sheppard, S.S., Vaduvescu, O., et al., 2008a. MPC 64484, 5.
- Benecchi, S., Sheppard, S.S., Vaduvescu, O., Pozo, F., Barr, A., Tudorica, A., Sonka, A., 2008b. MPC 64096, 9.
- Benecchi, S., Sheppard, S.S., Vaduvescu, O., et al., 2009a. MPC 66688, 10.
- Benecchi, S., Sheppard, S.S., Vaduvescu, O., et al., 2009b. MPC 64753, 3.
- Benner, L., 2010. Private communication.
- Birlan, M., et al., 2010. *Astronomy & Astrophysics* 511, A40.
- Boattini, A., et al., 2003. *Earth, Moon and Planets* 93, 239.
- Boattini, A., et al., 2004. *Astronomy & Astrophysics* 418, 743.
- Bowell, E., Muinonen, K., 1994. In: *Hazards due to Comets and Asteroids*, p. 149.
- Bowell, E., 2011. ASTORB database: <<ftp://ftp.lowell.edu/pub/elgb/astorb.html>>.
- Cavadore, C., Vaduvescu, O., Birlan, M., Tudorica, A., Toma, R., Sonka, A., Opriseanu, C., Vidican, D., et al., 2008. MPC 63369, 9.
- EARN, 2011. Near Earth Asteroids Data-Base: <<http://earn.dlr.de/nea/>>.
- Elst, E.W., Masi, G., Lagerkvist, C.-I., Boattini, A., Behrend, R., Vaduvescu, O., 2008a. MPC 63591, 10.
- Elst, E.W., Lagerkvist, C.-I., Boattini, A., Vaduvescu, O., Greco, C., Behrend, R., 2008b. MPC 63129, 5.
- Elst, E.W., Lagerkvist, C.-I., Boattini, A., Boehnhardt, H., Vaduvescu, O., 2008c. MPC 62871, 8.
- Elst, E.W., Vaduvescu, O., Birlan, M., Tudorica, A., Toma, R., Sonka, A., Opriseanu, C., Vancea, C., Vidican, D., 2008d. MPC 62573, 3.
- Elst, E.W., Lagerkvist, C.-I., Boattini, A., Vaduvescu, O., 2009a. MPC 66195, 4.
- Elst, E.W., Lagerkvist, C.-I., Boattini, A., Vaduvescu, O., 2009b. MPC 65331, 2.
- Elst, E.W., Masi, G., Lagerkvist, C.-I., Boattini, A., Behrend, R., Vaduvescu, O., 2009c. MPC 65045, 7.
- EURONEAR, 2011. Observing Tools—Planning NEA Observations: <<http://euro.near.imcce.fr/tiki-index.php?page=Planning>>.
- Fitzsimmons, A., Vaduvescu, O., Asher, D., 2009a. MPC 66457, 4.
- Fitzsimmons, A., Vaduvescu, O., Tudorica, A., Badea, M., 2009b. MPC 65927, 9.
- Fitzsimmons, A., Vaduvescu, O., Tudorica, A., 2009c. MPC 65332, 1.
- Grav, T., 2009. Communication on the MPML discussion list.
- Gray, B., 2011a. FIND_ORB: <http://www.projectpluto.com/find_orb.htm>.
- Gray, B., 2011b. SAT_ID Software: <http://www.projectpluto.com/sat_id.htm>.
- Holman, M., Fitzsimmons, A., Grav, T., Vaduvescu, O., 2009. MPC 66196, 2.
- Holvorcem, P.R., Schwartz, M., Vaduvescu, O., Tudorica, A., Dumitru, D., 2010. MPEC 2010-E39.
- IMCCE, 2011. Ephemerides: <<http://www.imcce.fr/en/ephemerides/>>.
- Jedicke, R., 1996. *Astronomical Journal* 111, 970.
- Kern, S.D., Sheppard, S.S., Vaduvescu, O., Schechter, P.L., 2008. MPC 63365, 10.
- Kern, S.D., Sheppard, S.S., Vaduvescu, O., Schechter, P.L., 2009. MPC 66190, 11.
- Kolena, J., 1999. Conversion of Asteroid Proper Motion to Distance from the Sun: <<http://www.phy.duke.edu/~kolena/asteroid.html>>.
- Milani, A., Gronchi, G.F., 2009. Theory of Orbit Determination.
- Minor Planet Center (MPC), 2011: <<http://minorplanetcenter.net/>>.
- Morbidelli, A., et al., 2002. In: *Asteroids III*, 409.
- NEODyS, 2011. Near Earth Objects—Dynamic Site: <<http://newton.dm.unipi.it/neodyS/>>.
- NASA & JPL, 2011. Near Earth Object Program: <<http://neo.jpl.nasa.gov/>>.
- Pozo, F., Barr, A., Vaduvescu, O., et al., 2008. MPEC, 2008-U48.
- Raab, H., 2011. Astrometrica Software: <<http://www.astrometrica.at>>.
- Ryan, E.R., et al., 2009. *The Astronomical Journal* 137, 5134.
- Smithsonian Astrophysical Observatory, 2011. SAOImage DS9: <<http://hea-www.harvard.edu/RD/ds9/>>.
- Schildknecht, T., 2007. Optical surveys for space debris. *Astronomy and Astrophysics Review* 14, 41–111.
- Scotti, J.V., Pozo, F., Barr, A., Vaduvescu, O., et al., 2008a. MPEC, 2008-U45.
- Scotti, J.V., Pozo, F., Barr, A., Vaduvescu, O., et al., 2008b. MPEC, 2008-U46.
- Sheppard, S.S., Vaduvescu, O., Galad, A., Tudorica, A., Nedelcu, A., Toma, R., Opriseanu, C., 2008. MPC 62258, 1.
- Skvarc, J., 2010a. Asteroid Residual Calculator: <<http://www.fitsblink.net/residuals/>>.
- Skvarc, J., 2010b. Identification of satellites from astrometric positions: <<http://www.fitsblink.net/satellites/>>.
- Tholen, D.L., Bernardi, F., Micheli, M., 2008a. AAS DPS Meeting 40, 434.
- Tholen, D.J., Vaduvescu, O., Birlan, M., Tudorica, A., Toma, R., Nedelcu, A., Sonka, A., Opriseanu, C., et al., 2008b. MPC 62262, 5.
- Tholen, D.J., Elst, E.W., Lagerkvist, C.-I., Boattini, A., Behrend, R., Vaduvescu, O., 2009. MPC 65636, 2.
- Tubbiolo, A.F., Vaduvescu, O., Tudorica, A., et al., 2008. MPEC, 2008-K66.
- Vaduvescu, O., Tudorica, A., 2008. MPC 63125, 6.
- Vaduvescu, O., 2009. How we discovered between 56 and 483 asteroids in 3 nights, Vega 129, iul 2009 (electronic magazine), Bucharest Astroclub (in Romanian) <<http://www.astroclubul.ro/index.php/revista-vega/anhiva-vega>>.
- Wiegert, P., et al., 2007. *Astronomical Journal* 133, 1609.
- Wiegert, P., 2011. Private communication.
- Yoshida, F., et al., 2003. *Publications of the Astronomical Society of Japan* 55, 701.
- Yoshida, F., Nakamura, T., 2007. *Planetary and Space Science* 55, 1113.
- Young, J., Vaduvescu, O., Tudorica, A., et al., 2008. MPEC, 2008-K63.